

The removal of turbidity and toxic metals in the AMD using a combination of saw dust, bentonite clay and synthetic $\text{CaMg}_2(\text{OH})_2$

I. O. Ntwampe^{a,b,*}

^a Ntwampe Trading & Projects (PTY) Ltd, 497 Broadacres, Fourways, Johannesburg, South Africa

^b Department of Chemical Engineering, University of Johannesburg, Doornfontein 2028, Johannesburg, South Africa

*Corresponding author. E-mail: ontwampe@gmail.com

ABSTRACT

Sets of experiments were conducted using 200 mL of synthetic acid mine drainage (AMD) into five 500 mL glass beakers, dosed with varying quantities of bentonite clay, saw dust and $\text{CaMg}_2(\text{OH})_2$ respectively and as a flocculent (bentonite clay, saw dust and $\text{CaMg}_2(\text{OH})_2$), mixed at 250 and 100 rpm for 2 and 10 mins respectively. The samples settled for 1 hour after which the pH, conductivity, turbidity, dissolved oxygen, oxidation reduction potential and toxic metals were measured. The turbidity removal of AMD samples treated with a flocculent (0–23 NTU) is lower compared to that of the samples treated with bentonite clay and saw dust (27–32 NTU). Results show 100% removal of Ni, moderate percentage removal of Fe and slightly lower percentage of Cu in treated AMD using a flocculent. Turbidity removal in treated AMD using a flocculent is higher compared to that of the samples treated with bentonite clay, saw dust or $\text{CaMg}_2(\text{OH})_2$. Treated AMD using flocculent has low Ca, Mg, Cl^- and SO_4^{2-} content (>84.8%). The SEM micrograph of the sludge of the sample with a combination of 1.5 bentonite clay, 1.5 g saw dust and 20 mL 0.025 M $\text{CaMg}_2(\text{OH})_2$ dosage shows optimal sorption of turbid materials.

Key words: AMD, dosage, flocculent, mixed, pH, settled

HIGHLIGHTS

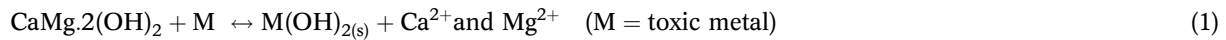
- Study utilises waste material.
- Treatment conducted without pH adjustment.
- Study removes total pollutants.
- Study utilises unprocessed reagents.
- Study utilises synthetic $\text{CaMg}_2(\text{OH})_2$ coagulant.

1. INTRODUCTION

Industrial expansion has been considered as one of the attributes to water pollution containing a variety of pollutants (Prabhu & Prabhu 2018), AMD being one of the wastewaters with detrimental effects to the environment. AMD is a type of wastewater that has been identified as the main environmental challenge which prevails in the mining industry particularly because of continuous decanting where conglomerate contains about 3% pyrite (Naicker *et al.* 2003). AMD also contains toxic metals and radioactive particles depending on the geochemistry and concentration level (Pérez-Esteban *et al.* 2013; Humby 2014; Bortonea *et al.* 2015). It poses a serious danger to the ecosystem due to toxic metal content. Its complex compounds; that is, toxic metals, total dissolved and suspended (TSS and TDS), organic and inorganic matter, odour and colour producing substances are the main attributes to problems associated with its treatment. Various technologies used include adsorption, precipitation, bioremediation, distillation, reverse osmosis, carbon nanotubes, Fenton's reagent, wet oxidation, and advanced oxidation, coagulation-electro oxidation (McCurdy *et al.* 2004; Swartz *et al.* 2004; Ghaly *et al.* 2006; Ntwampe *et al.* 2013; Skousen 2014; Chen *et al.* 2015; Liu *et al.* 2015; Mackie & Walsh 2015; Nel *et al.* 2014; Ntwampe *et al.* 2015a, Ntwampe *et al.* 2016; Demers *et al.* 2017; Ntwampe *et al.* 2017; Neelaveni *et al.* 2019), some being effective in toxic metal removal (Wu *et al.* 2011). Different types of reagents (organic or inorganic coagulants, metal hydroxides, biomass wastes, minerals, etc.) have been exploited to investigate a cost-effective technology, but that still remains a challenge. Considering all effective technologies employable in AMD treatment, adsorption has been identified as the most cost-effective method (Ntwampe 2013; Ntwampe *et al.* 2015b). The present study investigates the removal of the toxic metals in the AMD sample particularly

This is an Open Access article distributed under the terms of the Creative Commons Attribution Licence (CC BY 4.0), which permits copying, adaptation and redistribution, provided the original work is properly cited (<http://creativecommons.org/licenses/by/4.0/>).

Fe, Cu, Ni and others that appear in a low concentration using a combination flocculent (combination of bentonite clay, sawdust and $\text{CaMg}_2(\text{OH})_2$). Despite the fact that studies have been conducted using some of the reagents employed in this study, the novelty is that they are dosed as unprocessed synthetic flocculent with 33% mass content to reduce both costs and detrimental effect apparent when dosed in pure form. Although $\text{CaMg}_2(\text{OH})_2$ is a commercial reagent, it constitutes a small fraction and also plays a prominent role as it elevates the pH of the solution, suppressing the solubility of the toxic metals, as shown by Equation (1).



In view of the fact that AMD consists of toxic metals, the role of the $\text{CaMg}_2(\text{OH})_2$ component in a flocculent is to suppress solubility of toxic metals present in a sample. AMD can cause pollution to areas far from the mining sites by overflowing during rainfall into the rivers and tributaries feeding the oceans with highly contaminated feed water, causing perturbation to terrestrial or aquatic organisms (Kuyucak *et al.* 2006; Fischel *et al.*, 2015), hence it became imperative to operate under certain conditions relating to waste disposal (Lucier & Gareau 2016; Li & Ji 2017; Tepanosyan *et al.* 2017; DWA 2018).

Saw dust is another constituent of the flocculent investigated in this study. It is a waste that is produced from industrial activities on woodwork, biomass. Woodwork contains economic constituents that include 40–55% cellulose, 18–29% hemicelluloses and 16–35% lignin depending on plant species (Lai *et al.* 2014; Langan *et al.* 2014; Zhao *et al.* 2012). The percentage constituents show that approximately 190 and 150 million tons of hemicellulose and lignin can be recovered from the biomass activities in the pulp and paper industries (Cesarino *et al.* 2012; Huang *et al.* 2016). The collaboration of bio-refinery with the pulp and paper industry can expand and promote bio-based economy and reduce the usage of substances which are attributed to climate change (Liu *et al.* 2015). Hemicellulose is mainly composed of xylan, which is an ideal source of pentose and hexose sugars (Li *et al.* 2014; Li *et al.* 2016). They can further be processed to produce furfural, alcohols, polymers and other chemicals. On the other hand, lignin can also be utilized to produce phenols, carbon fibre, binders etc. or directly as a source of fuel due to its relatively high heating value (27 MJ/kg) (Baktash *et al.* 2015).

On the other hand, bentonite clay is an ideal adsorbent due to its plasticity and porous structure. It consists predominantly of a variety of minerals, mainly feldspars, montmorillonite, smectite, siliceous rocks, and glassy volcanic ash, depending on geological composition (Vermeulen 2012). Bentonite clay consists of different chemical compositions and a variety of minerals, such as montmorillonite, which contains the mineral group referred to as smectite known for a high cation-exchange potential and high swelling characteristic. The smectite group provides the montmorillonite with a crystalline appearance, which also exists in two major groups, namely dioctahedral and trioctahedral (Vermeulen 2012). The swelling property of the clay increases its surface area, resulting in permeability and spongy characteristics. A high permeability of a main compound is a determinant of a higher cation exchange capacity (CEC) associated with clay, explained as an ability of the compound (montmorillonite) to attract cations, a measurement of the net negative charge of the particles of the clay (Vermeulen 2012). Kaoline is another common mineral present in bentonite clay, and this contains a high concentration of Si and Al, which can react with certain elements such as sodium to form products that melt at high temperature (Kerr 1937). That also provides the main compound with a catalytic property, mainly during coal (containing clay minerals) combustion.

The performance of wastewater treatment is determined by the destabilizing-hydrolysis potential of the reagent(s), as was revealed by the study conducted by Ntwampe *et al.* (2013). Destabilization and hydrolysis are two reactions which co-exist, with the former occurring on the colloidal suspension and the latter on the coagulant(s); that is, metal ions of the salt (coagulant). It has also been stated that effective destabilization-hydrolysis is influenced by the physico-chemical properties of a metal ion; that is, high valence and electronegativity (Peavy *et al.* 1985). In the context of this study, Mg^{2+} has slightly inferior physico-chemical properties compared to those with superior properties such as Fe^{3+} and Al^{3+} ions. The present study also investigated the destabilizing-hydrolysis potential of $\text{CaMg}_2(\text{OH})_2$.

The objective of the present study was to determine sorption capacity of a combination of bentonite clay, saw dust and $\text{CaMg}_2(\text{OH})_2$ when added to the AMD sample to remove turbid materials, cations and toxic metals. Another objective was to determine the effect of $\text{CaMg}_2(\text{OH})_2$ during destabilization-hydrolysis and suppression

of solubility of toxic metals during AMD treatment without pH adjustment. A third objective was to compare adsorption capacity between bentonite clay and saw dust in a mixture of synthetic $\text{CaMg}_2(\text{OH})_2$.

2. MATERIALS AND METHODS

The AMD was synthesized by altering the concentration of toxic metals by adding 1.2 g of $\text{FeSO}_4 \cdot 7\text{H}_2\text{O}$, $\text{CuSO}_4 \cdot 5\text{H}_2\text{O}$ and $\text{NiSO}_4 \cdot 6\text{H}_2\text{O}$ respectively. The quantities of toxic metal compounds were diluted using 1 litre of demineralized water to the mark in the laboratory at the University of Johannesburg in South Africa. Elemental concentration of the mixture was measured using ICP-OES as shown in Table 1. The standard solutions were kept in a refrigerator to keep them inactive. The removal efficiency of turbid materials from the AMD was investigated by the addition of bentonite clay, saw dust and magnesium hydroxide, increasing one reagent while keeping the other constant, and vice versa using a jar test. Another set of experiments includes the dosage of a combination of bentonite clay, saw dust and $\text{CaMg}_2(\text{OH})_2$.

Table 1 | Properties of the AMD sample

Parameter	Exp. A	Exp. B	Exp. C
Temperature (°C)	21,5	23,5	24,9
pH	3,20	3,3	3,33
Conductivity (mS/cm)	5.76	5.79	5.78
ORP (mV)	212	201	203
Fe (ppm)	933	933	933
Cu (ppm)	345	345	345
Ni (ppm)	312	312	312
Co (ppm)	11.4	11.4	11.4
Se (ppm)	9.72	9.72	9.72
Zn (ppm)	8.22	8.22	8.22
Pb (ppm)	7.86	7.86	7.86
Ca (ppm)	193	193	193
Mg (ppm)	89	89	89
Cl^- (ppm)	212	212	212
SO_4^{2-} (ppm)	1,627	1,627	1,627

2.1. AMD sample

The samples were collected from the Western Decant in Krugersdorp in a 25 litre plastic drum. The sample was air-tied and stored at room temperature. The pH, conductivity, turbidity (TSS) and oxidation reduction potential (ORP) of untreated AMD sample were 2.22, 5.91 mS/cm, 256 NTU (875.5 g/L) and 243 mV respectively. Other parameters of the AMD including toxic metals are shown in Table 1.

2.2. Bentonite clay

Bentonite clay was obtained from a the Yellowstar Bentonite mine, a bentonite mining and supplying company situated in Parys in the Free State (SA). The bentonite was mined from a quarry located in Koppies (SA). The pH, conductivity, TSS, DO and ORP of bentonite clay were 2.15, 2.66 mS/cm, 13.5 g/L, 5.8 mg/L and 230 mV respectively.

2.3. Sawdust

The saw dust was collected from a carpentry workshop situated at the University of Johannesburg, South Africa. The particle size was already in the required conditions for the study. The sample was rinsed with demineralized water until there was no colour shown by the rinsing water.

2.4. Standard solution

Synthetic standard solution for preparation of 0.05 M of $\text{Ca}^{2+}/\text{Mg}^{2+}$ in $\text{CaMg}_2(\text{OH})_2$ which was dosed during treatment was accomplished by a mixture analytical grade of 1.85 g of $\text{Ca}(\text{OH})_2$ and 1.46 g of $\text{Mg}(\text{OH})_2$ in a litre of demineralised water as calculated in Equation (2). The mixture was shaken using a shaker at 300 rpm for 4 h, and the concentrations were obtained from the study by Ntwampe *et al.* (2017).

$$0.05 \text{ M of } \text{Ca}^{2+}/\text{Mg}^{2+} \times \text{mass of } \text{M}^*(\text{OH})_2 \quad (\text{M} = \text{Ca/Mg}) \quad (2)$$

3. EXPERIMENTAL METHODS

3.1. Jar test procedure

The equipment used for the jar tests was a BIBBY Stuart Scientific Flocculator (SW1 model), which has six adjustable paddles with rotating speeds between 0 and 250 rpm. The experiments were conducted employing rapid and slow mixing (250 and 100 rpm for 2 and 10 mins respectively). The experiments were conducted in the following order.

A total of 200 mL of a sample was poured into five 500 mL glass beaker and dosed with 1.0–3.0 g of bentonite clay and 1.0–3.0 g saw dust respectively; the samples were mixed at 250 and 100 rpm for 2 and 10 mins respectively, allowed to settle for 1 hour, after which the pH, conductivity, ORP and percent removal were measured. A second similar set of experiments was conducted with increasing dosage of bentonite clay (1.0–3.0 g) and constant saw dust (2.0 g) considering only quantitative parameter, similar treatment and measurement were conducted. A third set of experiments was conducted with increasing saw dust and constant bentonite clay, similar treatment and measurements were conducted, and vice versa, $\text{CaMg}_2(\text{OH})_2$ dosage was done in an increasing trend; that is, 20–60 mL.

3.2. Performance evaluation

3.2.1. pH, conductivity, DO and ORP measurements

A MettlerToledo Seven Multimetric instrument (made in Germany) was used to measure the pH, conductivity and ORP. Each measurement has its corresponding electrode filled with a solution of silver chloride solution and the outer glass casing, which has a small membrane covering at the tip. The instrument was calibrated daily prior to the experiments, and contained standard solutions of pH 4.0 and 7.0. An appropriate probe was placed prior to the analyses and a relevant measurement was selected using an appropriate button. The reading appeared on the instrument and was allowed to stabilize before the reading was recorded.

3.2.2. Turbidity measurement

A Merck Turbiquant 3000T Turbidimeter (made in Japan) was used to determine turbidity of the AMD using NTU as a unit of measure. Each piece of equipment was calibrated with 0.10, 0, 100, 1,000 and 10,000 NTU standard solutions.

3.2.3. Analytical method

3.2.3.1. Inductively coupled plasma (ICP). A Perkin Elmer Optima DV 7000 ICP-OES Optical Emission Spectroscopy (made in USA) was used to measure the concentration of toxic metals in the supernatant. Based on the anticipation of a high concentration of the heavy metals, the ICP equipment was calibrated with the standard solution between 100 and 1,000 ppm of the salts.

3.2.3.2. Ion chromatographic method. Ion chromatography Dionex ICS 5000 (Sunnyvale, made in US) equipped with IonPac AS12-AS anion column and suppressed conductivity detector to measure the chlorides and sulphates.

3.2.4. Characterization

Scanning electron microscopic analysis

A KYKY-EM3200 digital scanning electron microscope (model EM3200) equipment (China) was used to produce the SEM photomicrographs.

3.2.5. Adsorption isotherm

Adsorption capacity of an adsorbate onto adsorbent; that is, turbid materials onto the flocculent was determined. Pseudo-first and second orders are common models (Equations (3) and (4)).

Pseudo first order model

$$\frac{dq_t}{dt} = k_1(q_e - q_t) \quad (3)$$

Pseudo second order model

$$\frac{dq_t}{dt} = k_2(q_e - q_t)^2 \quad (4)$$

where q_e is the adsorbed amount of the turbid materials at equilibrium (mg/g), q_t is the adsorbed amount of turbid materials at a certain time t (mg/g) and k_1 and k_2 are the rate constants for the first and second order adsorption kinetics, respectively. Non-linear regression methods were used to determine these rate constants.

4. RESULTS AND DISCUSSION

The study investigates the removal efficiency of turbidity, toxic metals predominantly Fe, Cu and Ni, and hardness present in the AMD sample using a flocculent consisting of a combination of bentonite clay, saw dust and $\text{CaMg}_2(\text{OH})_2$ without the addition of neutralizing agents. Although bentonite clay and saw dust are known for their large surface area and water holding capacity, and indication of high adsorption capacity of turbid materials; optimal removal of pollutants cannot be guaranteed. Synthetic $\text{CaMg}_2(\text{OH})_2$ was added in the flocculent to increase its physico-chemical removal capacity. The study constitutes a major contribution in the scientific field as it investigates a treatment system utilizing a combination of naturally occurring minerals and waste materials without processing. A complexity of the chemical and mineral composition of clays and structural configuration is an attribute to its reactivity. The other factors that contribute towards the reactivity of clay include complex chemical structures, structural imperfections, varying crystallinity and the presence of impurities.

Figure 1 shows the relation between the pH, conductivity and ORP of the AMD sample treated with a flocculent (bentonite clay, saw dust and $\text{CaMg}_2(\text{OH})_2$) (exp. C), whereas Figures A1 and A2 (Exps A and B) show the relation between the pH, conductivity and ORP of the samples dosed with a combination of bentonite clay and $\text{CaMg}_2(\text{OH})_2$, and a combination of saw dust and $\text{CaMg}_2(\text{OH})_2$ respectively.

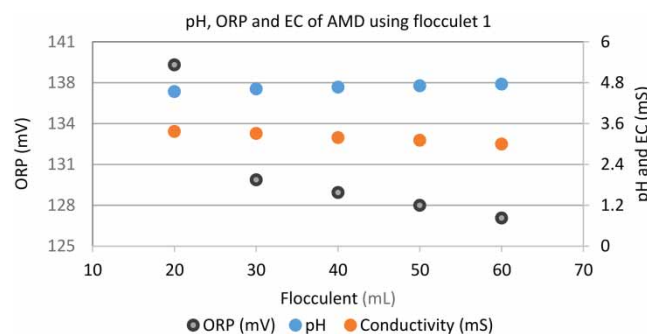


Figure 1 | pH, ORP and conductivity of AMD using flocculent 1.

The parameters above play a pivotal role during destabilization-hydrolysis, reflecting the rate at which the flocculent destabilises and hydrolyses the samples, the oxidation and reaction rate of the solution. The results are also indicative of the effect of ionic strength (electrical conductivity) and the rate of redox in the system. Destabilization potential; that is, reactivity strength of the flocculent, determines the ability of a flocculent to perturb equilibrium between the van der Waals attractive and electrostatic repulsive forces, screening effect between ions of similar charges, selective sorption of some cations/anions in a solution.

The pH of the samples using a flocculent increased from 2.22 to a range 4.72–4.98, indicating that dehydroxylation occurred during hydrolysis, a process whereby hydroxide ions are released into the system particularly by

$\text{CaMg}_2(\text{OH})_2$. In a situation of such a nature, increasing pH is considered attributed to the rate of adsorption of most of the pollutants, particularly those that dissolved in acidic suspension. The changing trend is already indicative of suppression of solubility of toxic metals to form precipitates of metal hydroxide.

The ORP of the samples was reduced from 243 mV to a decreasing trend in a range of 139–127 mV. The changing trend indicates that oxidation of toxic metals and other cations took place, enabling the hydroxylation process. Such a reaction also invokes the observations afore-mentioned regarding the removal of pollutants; that is, particularly toxic metals.

Electron conductivity of the samples was reduced from 5.91 mS/cm to a slight decreasing trend in a range of 3.57–3.05 mS/cm. The observation is an indication of the rate of internal reactions that occurred in the system. High ionic strength in a system effectively screens electrostatic forces of repulsion and reduces the distance between the particles, resulting in increasing effect of van der Waals forces of attraction (Gregory & Duan 2001). The observation already exhibits that a flocculent used in this experimental work has a high destabilizing potential (Ntwampe 2013).

Figs. A1 and A2 represent the pH, conductivity and ORP of the AMD samples treated with a combination of bentonite and $\text{CaMg}_2(\text{OH})_2$, and a combination of saw dust and $\text{CaMg}_2(\text{OH})_2$ respectively. According to Fig. A1, the pH showed an increasing trend with increasing $\text{CaMg}_2(\text{OH})_2$ in a range 4.4–4.8, decreasing conductivity and ORP in the ranges 3.13–2.75 mS/cm and 136–123 mV respectively. On the other hand, the pH (Fig. A2) showed an increasing trend of a range 4.23–4.38, whereas conductivity and ORP showed a decreasing trend in the ranges 3.30–2.86 and 156–120 mV respectively. The observations revealed by the ORP (Figs. A1 and A2) showed that oxidation was a predominant reaction as the trend decreased with increasing $\text{CaMg}_2(\text{OH})_2$ dosage. Decreasing conductivity exhibited by both graphs is indicative of the removal of ionic minerals in the AMD. On the other hand, the pH changing trend of Fig. A1 is slightly higher compared to that of Fig. A2, which is indicative of suppressed neutralization of bentonite clay compared to that yielded by saw dust (Fig. A2).

Figure 2 shows the relation between the pH, conductivity and residual turbidity of the AMD using bentonite clay, saw dust and flocculent respectively. The objective of this investigation was to determine the efficiencies of the saw dust and bentonite clay in the treatment of the AMD without the addition of a neutralizing agent.

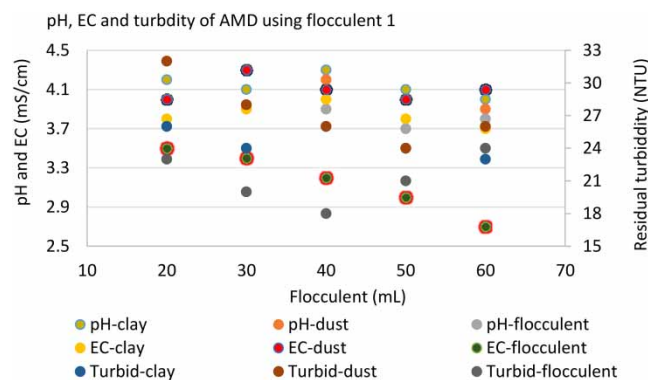


Figure 2 | Relation between the pH, conductivity, turbidity and ORP of AMD using flocculent 1.

The pH of the samples using bentonite clay, saw dust and a flocculent changed in the ranges 4.1–4.3, 3.1–3.8 and 3.0–3.5 respectively. According to the observations; that is, pH changing trend, reaction rate in the sample using a flocculent is faster compared to that of the samples using bentonite clay and saw dust respectively. Such an inference is based on a significant pH change between raw sample and treated effluent of the AMD using a flocculent and insignificant pH change using bentonite clay and saw dust. The corresponding conductivity of the samples with the same sequence of dosage is in the ranges 3.7–4.0, 4.0–4.3 and 2.7–3.5 mS/cm; however, the conductivity of the samples using flocculent is lower compared to that of the samples using bentonite clay and saw dust respectively. Such an observation invokes the statement which stated that $\text{CaMg}_2(\text{OH})_2$ component plays a pivotal role during the destabilization-hydrolysis process. However, conductivity of the samples using bentonite clay is slightly lower compared to that of the samples using saw dust. It is suggested that the ionic surface

property and porosity of bentonite clay (Vermeulen 2012) reacted with a fraction of ionic salts attributed to electrical conductivity of a samples.

On the other hand, the residual turbidity of the dosage in the same sequence changed inconsistently from 314 NTU (raw AMD) to the ranges 23–26, 24–32 and 18–24 NTU. The residual turbidity of the samples using bentonite clay is higher than that of the other two reagents, whereas residual turbidity of the samples using a flocculent is the lowest, 18–24 NTU. This observation shows that the three reagents in a flocculent are complimentary to one another; that is, bentonite clay and saw dust being effective in adsorption mechanism while $\text{CaMg}_2(\text{OH})_2$ in the suppression of the solubility of toxic metals to form settleable metal hydroxide compounds. It is also suggested that oxidation of toxic metals observed from low residual turbidity is attributed to reduction reaction of the Ca^{2+} and Mg^{2+} ions component of $\text{CaMg}_2(\text{OH})_2$ in a flocculent. This also includes their involvement during destabilization of the suspension due to their bivalent property, as stated in the study by Water Specialist Technology (2003) that both bivalent and trivalent cations have high destabilizing potential influential during hydrolysis electronegativity. On the other hand, large surface area, electrical conductivity, large exchange capacity (Syafalni *et al.* 2013) and T-O-T structural configuration of the bentonite clay are attributed to high removal of pollutants (absorption) (Ntwampe 2016). On the other hand, the removal of pollutants through intercalation is another factor that ameliorated the performance of the bentonite clay, enhancing its removal efficiency. The pH of a solution; that is, above two, is another attribute to optimal removal of pollutants, an inference invoked by the observation from a study (Ijagbemi *et al.* 2009) showing that maximum adsorption occurs above the pH of 2 and increases until it reaches 4.5 (pH in Figure 2). Another major contributor towards the removal efficiency of pollutants using bentonite clay is based on the system's acid activation by the protons present in the AMD, whereby ionic exchange occurs between the protons and Na^+ , K^+ , Ca^{2+} and Mg^{2+} in the bentonite layer; an observation invoked by the findings from the study conducted by Ntwampe *et al.* (2014). During the process, the interlayer bonding energy is reduced and the interlayer spacing and specific surface area of bentonite are increased (Cui *et al.* 1998; EBPA 2015), rendering the flocculent a better removal efficiency. On the other hand, the presence of sulphate ions in the solution activates the efficiency of bentonite clay to render the best activation effect. Acidic content of AMD also acts as a performance enhancement attribute by loosening a dense layered structure of bentonite, resulting in increasing interlayer spacing (Dong *et al.* 2019), key physicochemical properties of bentonite clay. The interlayer spacing of bentonite increases during cation exchange resulting in the interaction of organic molecules/compounds with hydroxyl groups on the surface of bentonite to form some new functional groups that change the local structure of bentonite clay (Chen *et al.* 2015). It is therefore suggested that most of the cationic compounds or pollutants are exchanged with the cations present in layers of bentonite clay, as revealed in the study by Chen *et al.* (2015). Figures 3 and 4 represent the relation between the removal efficiencies of Fe, Cu and Ni from the AMD sample using a flocculent (1.0 g bentonite clay, 1.0 g saw dust and 0.025 M $\text{CaMg}_2(\text{OH})_2$) and a combination of 1.0 g saw dust and 0.025 M $\text{CaMg}_2(\text{OH})_2$ respectively. The rationale of the comparison was to determine the effect of a combination of saw dust and $\text{CaMg}_2(\text{OH})_2$ in a flocculent for the removal of toxic metals (Fe, Cu and Ni) and Co, Se, Pb and Zn.

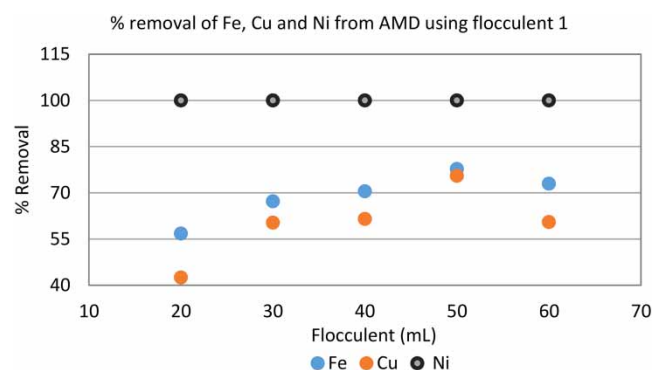


Figure 3 | % Removal of Fe, Cu and Ni from the AMD using flocculent 1.

The results (Figure 3) showed high removal of Ni in the samples using a flocculent was from 314 ppm (raw AMD) to yield 100% removal efficiency. The results of the samples using a flocculent showed lower removal of Fe and Cu, where the former showed removal efficiency from 933 ppm to a range 55–82% and Cu showed

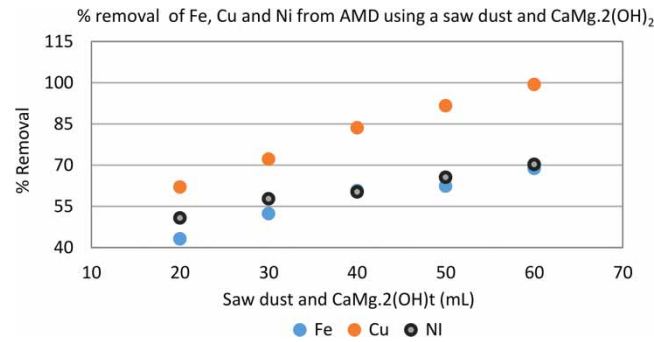


Figure 4 | % Removal of Fe, Cu and Ni from the AMD using flocculent 1.

removal efficiency from 345 ppm to a range of 40–81% removal efficiency. However, the sample with 20 mL of a flocculent yielded the lowest removal efficiency of 42% whereas 50 mL dosage yielded the highest removal efficiency of 81%. According to the physico-chemical properties of the constituents of a flocculent (bentonite clay, saw dust and $\text{CaMg}_2(\text{OH})_2$), which include high ionic exchange, porosity, high swelling, high electronegativity (high destabilization-hydrolysis) and high solubility suppressing capacity; it is suggested that Ni responded positively towards those properties. This indicates that Ni is easily insolubilized by basic neutralizing agents ($\text{CaMg}_2(\text{OH})_2$), hence high removal efficiency due to the formation of precipitates which settled easily; whereas both Fe and Cu showed a moderate reactivity compared to Ni. On the other hand, the same reagent showed a high destabilization-hydrolysis potential, resulting in the formation of the flocs which are either sorption substrates or settled easily. Based on high ionic exchange and porosity of bentonite clay and saw dust, it is suggested that Ni showed high sorption onto both reagents and ionic exchange, which indicates that it has high physico-chemical reactive potential. The results showed that the reactions of both Fe and Cu were moderate. On the other hand, calcium and magnesium in the AMD were reduced from 93, 89 ppm (Table 1) to the ranges of 45–47, 32–39 ppm respectively (Table 2).

On the other hand chlorides and sulphides which have a negative effect in aquatic environment constituting mainly to corrosion and scaling; where the sulphides produced under anaerobic condition results in oxygen deficiency which is detrimental to aquatic life (Geurts *et al.* 2009). Chlorides and sulphates were reduced considerably from 212 and 1,627 ppm (raw AMD) to 91–99 and 449–465 ppm respectively. The observation shows that a flocculent exhibited optimal removal of calcium, magnesium, chlorides and sulphates. The removal of chlorides and sulphates, permanent hardness, revealed in this study exhibited a distinctive observation relating to removal efficiency of salts attributed to water hardness as are not easily removed compared to those attributed to temporary water hardness. Toxic metal with low concentration, i.e. Co, Se, Pb and Zn are reduced from 11.4, 9.72, 8.22 and 7.86 ppm (raw AMD) (Table 1) to the ranges of 2.97–3.11, 1.81–1.96, 0.73–1.07 and 1.11–1.28 ppm respectively (Table 2). The results shows optimal removal of toxic metals occurred at pH in a range 2.7–3.6, which indicates that efficiency of a flocculent used in the experiment operates optimally in that range. The flocculent showed a relatively high removal efficiency of the toxic metal present in low concentrations, which is also

Table 2 | Salt content of treated AMD using flocculent 1

Parameter	Exp A	Exp B	Exp C
Co (ppm)	3.11	3.01	2.97
Se (ppm)	1.89	1.96	1.81
Pb (ppm)	0.87	1.07	0.73
Zn (ppm)	1.28	1.11	1.19
Ca (ppm)	47	50	45
Mg (ppm)	32	36	39
Cl^- (ppm)	96	91	99
SO_4^{2-} (ppm)	465	454	449

attributed to solubility suppression by the $\text{CaMg}_2(\text{OH})_2$ and sorption capacity of both bentonite clay and saw dust including intercalation and co-precipitation by primary flocs (Aboulhassan *et al.* 2006). On the other hand, there is a propensity that the composite of saw dust with bentonite significantly ameliorated the spacing between the bentonite layers, improved the pore structure, swelling and sorption of the composite to avoid agglomeration, as revealed in the studies conducted by Neelaveni *et al.* (2019) and Sato *et al.* (2016) using graphite and polymer combined with bentonite clay respectively.

The removal efficiencies of Fe from the AMD sample using a combination of saw dust clay and $\text{CaMg}_2(\text{OH})_2$ changed from a concentration of 933 ppm (raw AMD) to an increasing percentage removal in a range 42–70%, those for Cu and Ni also exhibit a change from 345 to 312 ppm to increasing percentage removal trends of 62–98 and 53–70% respectively. The results show that a flocculent has a high percentage removal for Cu and almost identical percentage removal for both Fe and Ni. According to the removal efficiencies of both flocculants (Figures 3 and 4), bentonite clay exhibited high efficiency for the removal for Ni, whereas saw dust exhibited the best efficiency for the removal for Cu. On the other hand, bentonite clay showed moderate efficiency on Fe and Cu removal whereas saw dust showed moderate removal efficiency for Fe and Ni.

Figure 5 shows the relation between the pH and % removal of Fe, Cu and Ni from AMD using a combination of 1.5 g bentonite clay, 1.5 g sawdust and increasing 0.025 M $\text{CaMg}_2(\text{OH})_2$ (flocculent 1) and 1.5 g bentonite clay, 1.5 g sawdust and increasing 0.05 M $\text{CaMg}_2(\text{OH})_2$ (flocculent 2). The selection of the dosage of the bentonite clay and saw dust was based on the results shown by their efficiencies in their respective flocculants (Figures 3 and 4).

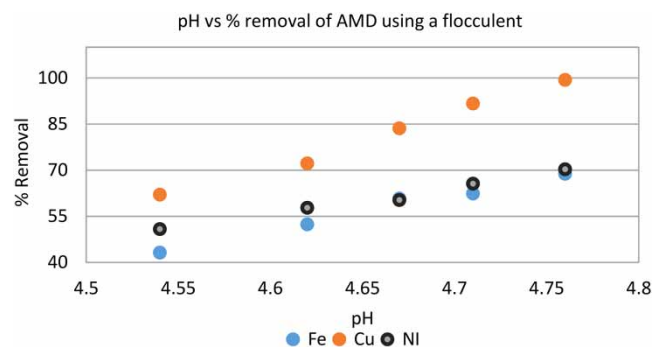


Figure 5 | pH vs % removal of Fe, Cu and Ni from AMD using flocculent 1.

The results of treated AMD (Figure 5) where a flocculent used consists of 1.5 g bentonite clay, 1.5 g saw dust and 0.025 M $\text{CaMg}_2(\text{OH})_2$ (flocculent 1) showed different removal efficiencies compared to those of the results shown in Figures 3 and 4. The inference is based on the increasing removal trend of all toxic metals (Fe, Cu and Ni), whereby removal efficiency of Cu is the highest, i.e. in an increasing trend of a range 62–100%, whereas those of Fe and Ni also showed an increasing trend in the ranges of 42–70 and 53–72% respectively. Unlike the results (Figure 3) showing that removal efficiency of Ni was 100%, the results shown in this diagram revealed that higher dosage of the flocculent yielded 92–100% removal efficiency. On a contrary, the removal efficiency of Ni (Figure 5) is in a range of 53–72% whereas removal efficiency of Fe is relatively close to that of the results obtained in Figure 3. The results showed quantitative consideration of bentonite clay and saw dust playing a pivotal role in the removal efficiency of toxic metals as changing the quantity of both reagents yielded different removal efficiencies of Fe, Cu and Ni. The main reason for varying removal efficiencies of various metals is based on the differing sizes of their radii, i.e. those with smaller hydration radius and stronger electronegativity can easily occupy adsorption sites on the adsorption substrate (flocculent of bentonite clay, saw dust and $\text{CaMg}_2(\text{OH})_2$). This simply implies that the competitive adsorption of the three toxic metal ions on a flocculent was multi-layer adsorption, and finally reached equilibrium condition variably (Tang *et al.* 2019).

Figure 6 shows Pseudo first order of the removal of Fe, Ni and Cu from AMD using a flocculent.

The coefficient regressions of the adsorption capacity for Fe, Cu and Ni from the AMD using a flocculent (Figure 6) applying pseudo first order model are 0.949 (94.9%), 0.963 (96.3%) and 0.925 (92.5%) respectively, indicating that the experimental data didn't fit well for the pseudo-first order model. However, the correlation

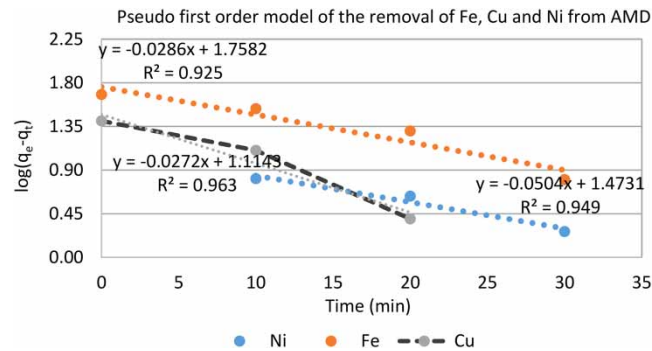


Figure 6 | Pseudo first order of the removal of Fe, Ni and Cu from AMD using flocculent 1.

regression of the removal efficiency for the Cu (96.3%) from the AMD sample applying pseudo first order can be deemed to fit as the point do not deflect much from the line.

Table 3 illustrates the pseudo first order parameters for the removal of Fe, Ni and Cu from the AMD using flocculent 1.

Table 3 | Pseudo first order of the removal of Fe, Ni and Cu using flocculent 1

Parameters	Fe	Ni	Cu
q_e (mg/g)	47,69851	11,08896	25,46753
q_e (mg/g)	6,330097	1,847209	2,497059
K1	0,065866	0,057805	0,116071

Figure 7 shows the Pseudo second order of the removal of Fe, Ni and Cu from AMD using flocculent 1.

The coefficient regressions of the adsorption capacity for Fe, Cu and Ni from the AMD dosed with flocculent 1 (Figure 6) applying the pseudo second order model are 1.0 (100%), 0.898 (89.8%) and 0.943 (94.3%) respectively, which indicates that the experimental data fit well for pseudo second order model for Ni and does not fit well for Fe and Cu.

Table 4 illustrates pseudo second order parameters for the removal of Fe, Ni and Cu from the AMD with a combination of bentonite clay and saw dust.

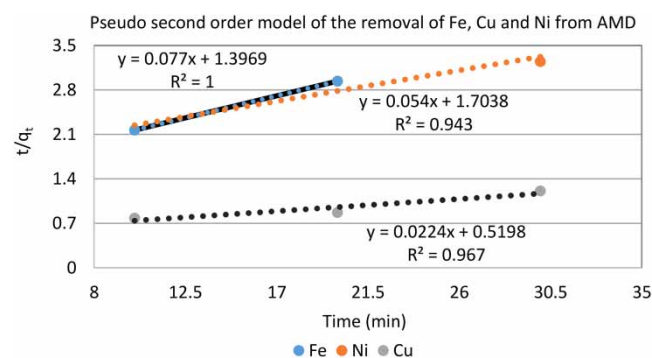


Figure 7 | Pseudo second order of the removal of Fe, Ni and Cu from AMD using flocculent 1.

Table 4 | Pseudo second order of the removal of Fe, Ni and Cu using flocculent 1

Parameters	Fe	Ni	Cu
q_e (mg/g)	12,98701	18,51852	46,72897
q_e (mg/g)	34,7115	7,429563	21,26144
K2	0,077	0,004244	0,00087

Figure 8 shows Freundlich model for Fe and Ni adsorption from AMD using flocculent 1.

Freundlich parameters for the removal of Fe and Ni from the AMD using flocculent 1 (Figure 8) yielded coefficient regressions 0.998 and 0.999 respectively, which is almost a unity. This shows that the model is an ideal fit for the experimental data. On the other hand, Langmuir parameters for the removal of Fe and Ni using flocculent 1 also yielded coefficient regressions 0.999 and 0.999 respectively. Both models are deemed as ideal fit for the experimental data. The R^2 values for both models is fall between 0 and 1, which is indicative of thermodynamic reactions.

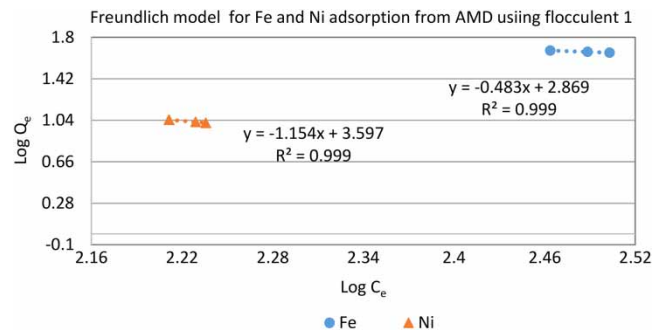


Figure 8 | Freundlich model for adsorption of Fe and Ni from the AMD using flocculent 1.

Figure 9(a) and 9(b) show the SEM micrographs of the dry sludge of a sample using flocculent 1 and that of a dry sludge of treated AMD sample using flocculent 2.

In Figure 9, slide 9A is a SEM micrograph of dry sludge of a sample using flocculent 1 showed dense sponge-like flocs suspended on a cluster formed by small flocs bonded together with filamentous structures. On the other hand, slide 9B is a dry sludge of a sample using flocculent 2 showed a dense sponge-like flocs surrounded by moderate size flocs. The former showing a surface with voids and porous morphological structure showing high plausibility of adsorption, whereas the latter exhibits filled pores appearing on the surface of the large and moderate structures around. The flocs with moderate size surrounding the large flocs are separated by voids which result from fragmentation during rapid mixing. The crystal morphology of both SEM micrographs show high sorption capacity which is a physico-chemical phenomenon, invoking high removal efficiency of toxic metals, turbidity and hardness observed in the results afore-mentioned.

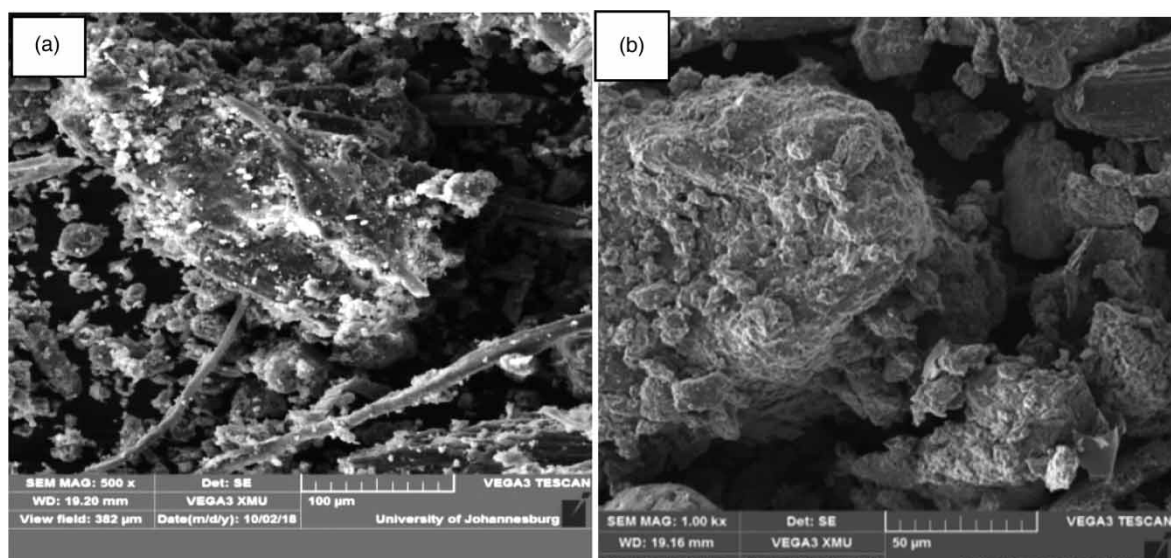


Figure 9 | SEM micrograph of dry sludge of a sample using flocculants 1 and 2.

5. CONCLUSION

The objective which includes the determination of the effect of unprocessed flocculent prepared by a combination of bentonite clay, saw dust and synthetic $\text{CaMg}_2(\text{OH})_2$. The study was conducted by comparing removal efficiency of pollutants, toxic metals and hardness in the AMD employing a jar test using a flocculent, bentonite clay, saw dust and $\text{CaMg}_2(\text{OH})_2$ respectively without pH adjustment. Based on individual physico-chemical properties of the three reagents used in the experiments, the results would show their complementary effects in a flocculent. The flocculent showed high efficiency for the removal of urbid materials, toxic metals and hardness. The flocculent has a neutralizing potential; that is, it caused a pH rise from 2.03 to a maximum of 4.8; and that was attributed to synthetic $\text{CaMg}_2(\text{OH})_2$. The flocculent has a high destabilizing and adsorption capacity shown by the removal of metals (cationic elements) and pollutants respectively, which also showed effective metal solubility suppression effects. The flocculent showed effective oxidizing potential, particularly to metallic elements indicated by decreasing trend of ORP.

Reducing trend of the conductivity of the samples shows that ionic strength of the flocculent has an effect on destabilization-hydrolysis, a precursor to floc formation and sorption. Bentonite clay has high removal efficiency for pollutants in AMD treatment compared to saw dust and $\text{CaMg}_2(\text{OH})_2$ respectively. Optimal performance of a flocculent during treatment indicates that the three reagents complement one another. Lower removal of pollutants using saw dust when compared with bentonite clay indicates that the former is originally saturated with reactive minerals such as cellulose, lignin and hydroxyl groups (tannins or phenolic compounds); active constituents in ion exchange and their electron-donating and electron-accepting nature causing perturbation to ionic exchange. On the other hand, the structural configuration of bentonite clay (T-O-T) is another factor contributory to its optimal removal efficiency, particularly by intercalation. Its swelling capacity, attributed to its porous property, is an ameliorating factor to its optimal turbid removal capacity. The crystal morphology of the flocculent (SEM) confirms that the composite of saw dust with bentonite significantly enhanced the physico-chemical abilities of a flocculent (spacing between the layers, pore structure, swelling and sorption) to achieve optimal removal of pollutants.

The flocculent has a high removal efficiency for Ni and moderate for Fe and Cu. Ni is easily insolubilized by basic neutralizing agents ($\text{CaMg}_2(\text{OH})_2$), resulting in high removal efficiency due to the formation of precipitates which settled easily. Bentonite clay dosage alone has a higher removal efficiency for Ni compared to saw dust, moderate efficiency for Fe and Cu, whereas saw dust showed moderate efficiency for the removal of Fe and Ni. Based on such inconsistent toxic metal removal capacity, it is imperative to pursue more research study to investigate the physico-chemical properties which cause such a changing trend. Synthetic $\text{CaMg}_2(\text{OH})_2$ exhibited a potential of enhancing removal efficiency of turbidity and toxic metals; however, more investigations on its physico-chemical properties attributable to its performance for the removal of pollutants in wastewaters is imperative. A flocculent consisting of 1.5 g bentonite clay, 1.5 g saw dust and 0.025 M $\text{CaMg}_2(\text{OH})_2$ exhibits high removal efficiency of turbid materials and toxic metals at pH in a range 2.7–3.6. Apart from the aforementioned research investigations, it is also imperative to pursue studies focusing on the cost-effectiveness of the both flocculants 1 and 2 using more toxic wastewaters such as discharge effluent from chemical and petrochemical industries, and saline water from the seas/ocean.

DATA AVAILABILITY STATEMENT

All relevant data are included in the paper or its Supplementary Information.

REFERENCES

- Aboulhassan, M. A., Souabi, S., Yaacoubi, A. & Baudu, M. 2006 [Removal of surfactant from industrial wastewaters by coagulation flocculation process](#). *Interface Journal of Environmental Science & Technology* **3**(4), 327–336.
- Baktash, E., Littlewood, P., Schomäcker, R., Thomas, A. & Stair, P. C. 2015 [Alumina coated nickel nanoparticles as a highly active catalyst for dry reforming of methane](#). *Applied Catalysis B: Environment* **179**, 122–127.
- Bortonea, I., Chianese, S., Ertoc, A., Di, A., Nardob, M. D. N., Santonastaso, G. F. & Musmarra, D. 2015 [Risk analysis for a contaminated site in North of Naples \(Italy\)](#). *Chemical Engineering* **43**, 777–780. doi:10.3303/CET1543322.
- Cesarino, I., Araújo, P., Domingues, J. A. P. & Mazzafera, P. 2012 [An overview of lignin metabolism and its effect on biomass recalcitrance](#). *Brazilian Journal of Botany* **35**, 303–311. doi: 10.1590/S0100-84042012000400003.
- Chen, Z., Wang, X., Ge, O. & Guo, G. 2015 [Iron oxide red wastewater treatment and recycling of iron-containing sludge](#). *Journal of Clean Products* **87**, 558–566. doi:10.1016/j.jclepro.2014.10.057.

- Cui, W. L., Zhang, C. Y. & Su, S. 1998 The feasible study on low class Ca bentonite to be activated and recreated. *China Non-Metallic Minerals Industry* **4**, 23–25.
- Demers, I., Mbonimpa, M., Benzaazoua, M., Bouda, M., Awoh, S., Lortie, S. & Gagnon, M. 2017 Use of acid mine drainage treatment sludge by combination with a natural soil as an oxygen barrier cover for mine waste reclamation: laboratory column tests and intermediate scale field tests. *Mineral Engineering* **107**, 43–52.
- Department of Water Affairs (DWA) 2018 *Feasibility Study for A Long-Term Solution to Address the Acid Mine Drainage Associated with the East, Central and West Rand Underground Mining Basins. Study Report No. 5.5: Options for the Sustainable Management and Use of Residue Products From the Treatment of AMD*. DWA Report No. P RSA 000/00/16512/5.
- Dong, H. H., Qi, R. S., Wang, X. H. & Zhao, Y. D. 2019 Effect of acid modification on structure and heavy metal adsorption properties of bentonite. *Non-Metallic Mines* **42**(02), 97–99. doi: CNKI:SUN:LGFK.0.1998-04-006.
- European Bentonite Producers Association (EBPA) 2015 *Bentonite*. IMA Europe Available from: <http://www.ima-europe.eu/about-industrial-minerals/industrial-minerals-ima-europe/bentonite> (accessed 6 November 2015).
- Fischel, M. H. H., Fischel, J. S., Lafferty, B. J. & Sparks, D. L. 2015 The influence of environmental conditions on kinetics of arsenite oxidation by manganese-oxides. *Geochemistry Transformation* **16**, 15. doi:10.1186/s12932-015-0030-4.
- Geurts, J. J. M., Sarneel, J. M., Willer, B. J. C., Roelofs, J. G. M., Verhousen, J. T. A. & Lamer, L. P. M. 2009 Interacting effects of sulphate pollution, sulphide toxicity and eutrophication on vegetation developments in ferns: a mesocosm experiment. *Environmental Pollution* **157**, 2072–2081.
- Ghaly, A. E., Snow, A. & Faber, B. E. 2006 Treatment of grease filter washwater by chemical coagulation. *Canadian Biosystems Engineering* **48**, 6.13–6.22.
- Gregory, J. & Duan, J. 2001 Hydrolyzing metal salts as coagulants. *Pure Applied Chemistry* **73**(12), 2017–2023.
- Huang, C., He, J., Min, D., Lai, C. & Yong, Q. 2016 Understanding the nonproductive enzyme adsorption and physicochemical properties of residual lignins in moso bamboo pretreated with sulfuric acid and kraft pulping. *Applied Biochemistry and Biotechnology* **180** (8), 1508–1523.
- Humby, T. 2014 Mining and the Environment: Legal framework, [lecture], Mining and the Environment, WITS University, CSMI, 4-5-6/3/2014.
- Ijagbemi, C. O., Baek, M. H. & Kim, D. S. 2009 Montmorillonite surface properties and sorption characteristics for heavy metal. *Journal of Hazardous Materials* **166**(1), 538–546.
- Kerr, P. F. 1937 Attapulgas clay. *American Mineral* **22**, 534–550.
- Kuyucak, N., Chabot, F. & Martschuk, J. 2006 Successful implementation and operation of a passive treatment system in extreme cold Northern Quebec. In: *Canada 7th ICARD Leadership: Gateway to the Future*.
- Lai, C., Tu, M., Li, M. & Yu, S. 2014 Remarkable solvent and extractable lignin effects on enzymatic digestibility of organosolvent-pretreated hardwood. *Bioresource Technology* **156**, 92–99. doi:10.1016/j.biortech.2014.01.030.
- Langan, P., Petridis, L., O'Neill, H. M., Pingali, S. V., Foston, M. & Nishiyama, Y. 2014 Common processes drive the thermochemical pretreatment of lignocellulosic biomass. *Green Chemistry* **16**, 63–68. 10.1039/C3GC41962B.
- Li, H. & Ji, H. 2017 Chemical speciation, vertical profile and human health risk assessment of heavy metals in soils from coal-mine brownfield, Beijing, China. *Journal of Geochemical Exploration* **183**, 22–32.
- Li, H., Pu, Y., Kumar, R., Ragauskas, A. J. & Wyman, C. E. 2014 Investigation of lignin deposition on cellulose during hydrothermal pre-treatment, its effect on cellulose hydrolysis, and underlying mechanisms. *Biotechnology and Bioengineering* **111**, 485–492. 10.1002/bit.25108.
- Li, Y., Qi, B., Luo, J. & Wan, Y. 2016 Effect of alkali lignins with different molecular weights from alkali pretreated rice straw hydrolyzate on enzymatic hydrolysis. *Bioresource Technology* **200**, 272–278. 10.1016/j.biortech.2015.10.038.
- Liu, A., Ren, F., Lin, W. Y. & Wang, J. Y. 2015 A review of municipal solid waste environmental standards with a focus on incinerator residues. *International Journal of Sustainable Built Environment* **4**, 165–188. doi:10.1016/j.ijbsbe.2015.11.002.
- Lucier, C. A. & Gareau, B. J. 2016 Obstacles to preserving precaution and equity in global hazardous waste regulation: an analysis of contested knowledge in the Basel convention. *International Environmental Agreement* **16**, 493–508. doi:10.1007/s10784-014-9261-6.
- Mackie, A. L. & Walsh, M. E. 2015 Investigation into the use of cement kiln dust in high density sludge (HDS) treatment of acid mine water. *Water Research* **85**, 443–450.
- McCurdy, K., Carlson, K. & Gregory, D. 2004 Floc morphology and cyclic shearing recovery: comparison of alum and polyaluminum chloride coagulants. *Water Research* **38**(2), 486–494.
- Naicker, K., Cukrowska, E. & McCarthy, T. S. 2003 Acid mine drainage arising from gold mining activity in Johannesburg, South Africa. *Environmental Pollution* **122**, 29–40.
- Neelaveni, M., Santhana, K. P., Ramya, R., Sonia, T. G. & Shanthi, K. 2019 Montmorillonite/graphene oxide nanocomposite as superior adsorbent for the adsorption of Rhodamine B and Nickel ion in binary system. *Advanced Powder Technology* **30**(3), 596–609. doi: 10.1016/j.apt.2018.12.005.
- Nel, M., Waander, F. B. & Fosso-Kankeu, E. 2014 Adsorption potential of bentonite and attapulgite clays applied for the desalination of sea water. In: *Conference Report. Cape Town: 6th International Conference on Green Technology. Renewable Energy & Environmental Engineering North-West University, RSA*.
- Ntwampe, I. O. 2013 *Treatment of Paint Wastewater Using Inorganic Coagulants*. A thesis submitted for PhD at the University of the Witwatersrand, RSA.

- Ntwampe, I. O., Jewell, L. L. & Glasser, D. 2013 The effect of water hardness on paint wastewater treatment by coagulation-flocculation. *Journal of Environmental Chemistry and Ecotoxicology* 5(1), 7–16.
- Ntwampe, I. O., Waanders, F. B., Fosso-Kankeu, E. & Bunt, J. R. 2014 Reactivity of Fe salts in the destabilization of acid mine drainage employing mixing and shaking techniques without pH adjustment. Accepted manuscript to *International Journal of Materials Processing. Journal of Environmental Science & Ecotoxicology* 5(3), 47–56.
- Ntwampe, I. O., Waanders, F. B., Bunt, J. R. & Fosso-Kankeu, E. 2015a Comparison between mixing and shaking technique during the destabilization-hydrolysis of acid mine drainage (AMD) using $\text{Ca}(\text{OH})_2$ and $\text{Mg}(\text{OH})_2$. *Journal Chemical Engineering & Materials, Science* 6(3), 15–33.
- Ntwampe, I. O., Waanders, F. B. & Bunt, J. R. 2015b Turbidity removal efficiency of clay and a synthetic af-PACI polymer of magnesium hydroxide in AMD treatment. *International Journal of Science* 4, 88–104.
- Ntwampe, I. O., Waanders, F. B. & Bunt, J. R. 2016 Reaction dynamics of iron and aluminium salts dosage in AMD using shaking as an alternative technique in the destabilization-hydrolysis process. *International Journal of Scientific Research* 4, 5–23.
- Ntwampe, I. O., Waanders, F. B. & Bunt, J. R. 2017 The effect of the bentonite clay constituents in a flocculent of FeCl_3 and $\text{CaMg}_2(\text{OH})_2$ during AMD treatment. *Journal of Chemical Engineering & Procedural Technology* 8(3), 1–8. doi: 10.4172/2157-7048.1000344, ISSN: 2157-7048.
- Ntwampe, I. O. 2016 *Comparison of Chemical Reactivity Between Inorganic and Synthetic Polymers in the Treatment of AMD*. A dissertation submitted for M.Eng. degree at the University of North-West, RSA.
- Peavy, H. S., Rowe, D. R. & Tchobanoglous, D. 1985 *Environmental Engineering*. McGraw-Hill, Singapore.
- Pérez-Esteban, J., Escolástico, C., Moliner, A. & Masaguer, A. 2013 Chemical speciation and mobilization of copper and zinc in naturally contaminated mine soils with citric and tartaric acids. *Chemosphere* 90(2), 276–283.
- Prabhu, P. P. & Prabhu, B. 2018, A review on removal of heavy metal ions from waste water using natural/ modified bentonite. MATEC Web of Conferences 144:02021. doi:10.1051/mateconf/201714402021.
- Sato, K., Barast, G., Razakamanantsoa, A. R., Irini, D. M., Katsumi, T. & Levacher, D. 2016 Comparison of prehydration and polymer adding effects on Na activated Ca-bentonite by free swell index test. *Applied Clay Science*. S0169131716304276. doi: 10.1016/j.clay.2016.10.009.
- Skousen, J. 2014 Overview of acid mine drainage treatment with chemicals. In: *Acid Mine Drainage, Rock Drainage, and Acid Sulfate Soils: Causes, Assessment, Prediction, Prevention, and Remediation* (Jacobs, J. A., Lehr, J. H. & Testa, S. M., eds). John Wiley & Sons, Inc., Hoboken, NJ, USA. doi:10.1002/9781118749197.ch29.
- Swartz, C. D., Morrison, I. R., Thebe, T., Engelbrecht, W. J., Cloete, V. B., Knott, M., Loewenthal, R. E. & Kruger, P. 2004 Characterisation and Chemical Removal of Organic Matter in South African Coloured Surface Waters. WRC Report No. 924/1/03. Water Research Commission, Pretoria, South Africa.
- Syafalni, R., Abdullah, R., Abustan, I. & Ibrahim, A. N. M. 2013 Waste water treatment using bentonite, the combination of bentonite-zeolite, bentonite-alum, and bentonite-limestone as adsorbent and coagulant. *International Journal of Environmental Science* 4(3), 2013.
- Tang, R., Wang, Z. K. & Liu, K. 2019 Competitive adsorption of Cu (II), Cd (II) and Mn (II) on organically modified magnetic bentonite. *Non-Metallic Mines* 42(04), 77–81. doi: 10.3969/j.issn.1000-8098.2019.04.024.
- Tepanosyan, G., Sahakyan, L., Belyaeva, O., Maghakyan, N. & Saghatelian, A. 2017 Human health risk assessment and riskiest heavy metal origin identification in urban soils of Yerevan, Armenia. *Chemosphere* 184, 1230–1240.
- Vermeulen, U. 2012 *Desorption of Heavy Metals From Bentonite Clay by Means of Sulphuric Acid Addition*. Bachelor Thesis, Potchefstroom: Faculty of Engineering North-West University, RSA.
- Water Specialist Technology 2003 *Jar Test Procedure for Precipitants, Coagulants & Flocculants*. Information Bulletin, Florida, USA.
- Wu, P., Zhang, Q., Dai, Y. & Zhu, N. 2011 Adsorption of Cu(II), Cd(II) and Cr(III) ions from aqueous solutions on humic acid modified Ca-montmorillonite. *Geoderma* 164, 215–219.
- Zhao, X.-T., Zeng, T., Li, X.-Y., Hu, Z. J., Gao, H.-G. & Xie, Z. 2012 Modeling and mechanism of the adsorption of copper ion onto natural bamboo sawdust. *Carbon Pollution* 89(1), 185–192.

First received 22 April 2021; accepted in revised form 22 July 2021. Available online 4 August 2021